Tectonophysics, 223 (1993) 15–37
Elsevier Science Publishers B.V., Amsterdam

Glacial rebound and sea-level change: an example of a relationship between mantle and surface processes

Kurt Lambeck

Institut de Physique du Globe de Paris, 4 Place Jussieu, 75005 Paris, France

(Received April 8, 1993; revised version accepted April 19, 1993)

ABSTRACT

Lambeck, K., 1993. Glacial rebound and sea-level change: an example of a relationship between mantle and surface processes. In: R. Wortel, U. Hansen and R. Sabadini (Editors), Relationships between Mantle Processes and Geological Processes at or near the Earth's Surface. *Tectonophysics*, 223: 15–37.

The problem of glacial rebound provides an outstanding example of the relationship between surface and mantle processes on time scales of 10^3 to 10^5 years. Changes in surface loading of ice and melt-water associated with the growth and decay of the great ice sheets deform the surface of the planet and induces flow in the mantle. A measure of the Earth's response to the changing surface loads and internal deformation is provided by observations of past sea levels relative to the present level, and inversion of these observations provides constraints on both the models of the rheological response of the Earth to loading and on models of the ice sheets. Constraints on ice sheet models include the total volume of the grounded ice at the time of maximum glaciation, the global rates of melting of the ice sheets, the thickness of the ice at maximum glaciation, the extent of ice cover over shallow seas such as the North Sea and the Barents Sea, and the role of Antarctica in the global ice balance. Constraints on mantle parameters include the effective lithospheric thickness and the effective viscosity of the mantle. Some recent results for both sets of parameters are discussed.

1. Introduction

This symposium addresses issues of the relationship(s) between mantle processes and geological processes at or near the surface of the Earth. I will be addressing one example of such a relationship between mantle deformations and surface processes that operate on a time scale of 10^3–10^5 years. This is the problem of glacial rebound and the concomitant change in sea level. Surface processes, in this case the waxing and waning of the great ice sheets during the Pleistocene, stress and deform the mantle by amounts that are observationally significant and which, through a feed-back mechanism, determine in part the volumes of ice that can be supported by the planet. The mantle part of the problem is the determination of the response of the Earth to changes in ice and water loads during the cycles of glaciation and deglaciation. The glaciological or surface problem is one of inferring from observations of this response constraints on models of the Late Pleistocene ice sheets. The geophysical problem is an important one because it provides one of the less ambiguous experiments for determining the Earth's response to forcing at periods longer than those achieved in the laboratory or inferred from seismology or geodesy measurements. A number of geophysical observations point to non-elastic behaviour of the Earth over a wide range of frequencies but no coherent description of this behaviour yet exists and one of the objectives of geophysics is to determine an appropriate relaxation function (or functions) that describes the behaviour of the Earth over a range of frequencies from seconds to 10^9 years. Thus,

On leave from Research School of Earth Sciences, Australian National University, Canberra, 2601 A.C.T., Australia

the glacial rebound results provide an important intermediary between the high-frequency seismic and geodetic observations and the low-frequency phenomena associated with mantle convection. The glaciological inferences that can be drawn from the study of the glacial rebound problem are important ones in that there are few, if any, direct measures of the ice volumes during the last glacial maximum and most estimates are based on ice flow laws, on models of ice accumulation and destruction, or on sparse and ambiguous geomorphological indicators.

The glacial rebound problem is hardly a new one. Already in the last century it had been suggested that the many elevated shorelines of Scotland, northern Europe and North America were the result of the Earth's adjustment to the removal of the Late Pleistocene ice sheets. Early attempts to infer mantle viscosities from these shorelines were made in the 1930's and 1940's by Haskell, Niskanen, Vening Meinesz, Gutenberg and others. In the past twenty-five years, starting with papers by McConnell (1968), O'Connell (1971) and Walcott (1972), the subject has enjoyed a type of renaissance because knowledge of the mantle viscosity structure is important for the quantification of processes of mantle convection. An important contribution to the subsequent development was the much improved formulation of the rebound problem, developed by Cathles (1975), Farrell and Clark (1976) and W.R. Peltier and colleagues (Peltier, 1974; Peltier and Andrews 1976; Clark et al., 1978). The application of this development has also been much aided by the improved computing facilities of the past few years which has permitted the calculation of more realistic solutions; solutions that treat the problem globally with much higher precision and with a greater spatial and temporal resolution than was previously possible, while at the same time permitting a considerably greater range of earth and ice models to be explored (e.g., Nakada and Lambeck, 1987; Tushingham and Peltier, 1991; Mitrovica and Peltier, 1991; Lambeck, 1991; Johnston, 1993).

The glacial rebound problem is an inverse problem in which a partially known forcing function (the time-dependent surface load of ice and meltwater) produces a deformation (the change in sea level relative to its present level) from which the earth structure (the mantle rheology) is inferred together with other parameters that constrain aspects of the ice models. Because of the complex temporal and spatial variability of the response, it does become possible to establish some separation of the parameters that describe both the Earth and the ice sheets such that the rebound model can provide a coherent framework for discussing past sea-level change and perhaps for providing insights into other geological processes such as recent vertical tectonics, the evolution of coastlines or the development of coral reefs.

Despite much progress in recent years, much of the work is still preliminary, with the emphasis having been more on establishing methodologies and numerical procedures and on improving the observational data base than on insisting on the finality of any of the results. However, the preliminary results are sufficiently interesting and promising to merit a review of some of these developments. Firstly, in this paper I summarize aspects of the sea-level equation that link the mantle processes to the surface processes. Next, some of the principal characteristics of the Earth's response, as reflected in changes in sea level or shoreline displacements, are discussed with emphasis on how it is possible to infer certain parameters describing aspects of both the Earth's rheology and the ice sheets. This is followed by a discussion of ice-sheet and earth-model inferences drawn from shoreline displacement data for different regions of the Earth.

2. The sea-level equation

The observed change in sea level usually takes the form of heights and ages of former shorelines above or below their present level. Under the influence of the glacial rebound and the associated hydro-isostasy (the adjustment of the crust to the changing water load), the relative sea-level change at a position φ and time t before the present can be schematically expressed as (Farrell

and Clark, 1976; Clark et al., 1978; Nakada and Lambeck, 1987):

$$\Delta\zeta(\varphi, t) = \Delta\zeta_e(t) + \Delta\zeta_i(\varphi, t) + \Delta\zeta_w(\varphi, t) \quad (1)$$

The first term on the right-hand side is the *equivalent* or eustatic *sea level* (esl) defined as:

$$\Delta\zeta_e(t) = (\rho_{ice} \times \text{change in ice volume})/(\rho_{water} \times \text{ocean surface area}) \quad (2)$$

(where ρ is density) and it provides a measure of the change in ice volume (other than floating ice) through time. The second term in eq.(1), the *ice-load* term $\Delta\zeta_i$, describes the incremental change in sea level that is associated with the deformation of the Earth resulting from the changing ice sheets. It includes the contribution from the change in the gravity field produced by both the changing mass distribution of the ice and by the redistributed mass within the mantle. This term will be a function of both the rheological model of the Earth and the temporal and spatial distribution of the ice sheets. The third term, the *water-load* term $\Delta\zeta_w$, defines the contribution to the changing sea level produced by the adjustment of the Earth to the redistributed water load resulting from the withdrawal of water from (or the addition of water to) the oceans as the ice sheets grow (or decay). It includes the contribution from the associated changes in the gravity field. It will be a function of the Earth's rheology, of the shape of the oceans and of the change in sea level itself. In formulating the two load functions, mass is conserved and the ocean surface remains an equipotential surface at all times. The solutions are usually obtained by expanding the surface loads and the ocean geometry into spherical harmonics such that the load terms in eq.(1) can be expressed schematically as:

$$\Delta\zeta(\varphi, t) = \Delta\zeta_e(t) + \sum_{n=0}^{n_{max}} \Delta\zeta_i^{(n)} + \sum_{m=0}^{m_{max}} \Delta\zeta_w^{(m)} \quad (3)$$

High-degree expansions of n_{max}, m_{max} equal to 180, or even 240 in some instances (Nakada and Lambeck, 1987; Lambeck, 1991), are required in order that the expansions have converged to a degree that is commensurate with observational accuracies. In most cases it will be necessary to consider the ice-load terms from a number j ($j = 1, \ldots, J$) of ice sheets and it will be convenient to write eqn (3) as:

$$\Delta\zeta(\varphi, t) = \Delta\zeta_e(t) + \sum_{j=1}^{J} \left\{ \sum_{n=0}^{n_{max}} \Delta\zeta_i^{(n)} + \sum_{m=0}^{m_{max}} \Delta\zeta_w^{(m,j)} \right\} \quad (4)$$

Because of the dependence of the water load term on the sea-level change itself, eq.(1) is an integral equation which can be solved iteratively and different approaches have been developed (Clark et al., 1978; Wu and Peltier, 1983; Mitrovica and Peltier, 1991; Johnston, 1993). A relatively simple and precise procedure, but one that is computationally expensive if carried out to a very high degree, is to obtain a first-iteration solution by evaluating the water-load term on the assumption that sea level is everywhere equal to the equivalent sea level, eq.(2). In the second iteration, the first-iteration solution for $\Delta\zeta(\varphi, t)$ is then substituted into the water-load integral $\Delta\zeta_w$ to obtain an improved estimate for the sea-level change. For locations far from the former ice sheets, where the water-load term is usually relatively small, the first-iteration solutions give reasonable results but for locations near or within the former ice sheet limits higher-order solutions are required if the predictions are to be precise to better than about 5–10%. The water-load term is also a function of the ocean geometry, which itself will be a function of the change in sea level, and recent solutions incorporate this dependence to varying degrees of precision (Lambeck and Nakada, 1990; Johnston, 1993).

The earth model is described by elastic parameters and density profiles derived from seismic models. In contrast, the viscosity profile is usually approximated by a number of discrete layers of different effective linear viscosities whose values are considered as unknowns to be inferred from the observational data. Strong lateral variations in the viscosity, particularly for the upper mantle, can be expected because of the evidence of lateral variations in temperature and the usually marked dependence of viscosity on temperature. Realistic lateral variations in mantle parameters

are, however, difficult to incorporate into the models because they are likely to occur rather abruptly, across continental margins for example, and because the observational data set is inadequate for a global analysis of regional structures. Instead, it may be possible to extract information on lateral structures by examining observations that are sensitive to a regional response and to compare mantle inferences for different regions (Nakada and Lambeck, 1991).

In the solutions of the sea-level equations discussed here, the response of the mantle to loading has been assumed to be fully non-adiabatic in the sense that any particle displaced to a new depth in a medium of depth-dependent density retains its original density and thereby experiences a buoyancy force. It has been pointed out by Cathles (1975) and Fjeldskaar and Cathles (1984) that adiabatic models may be more appropriate when the mantle is chemically homogeneous or at phase-transition boundaries with the result that displaced particles blend with the material at their new depth and experience no buoyancy. The solutions by Peltier and colleagues, as well as those by Lambeck and Nakada, are generally based on the non-adiabatic assumption, largely for reasons of convenience, but recent adiabatic solutions have been developed by P. Johnston and it has been possible to estimate the effect of this assumption on the model parameters. This is discussed further below.

All observations used to constrain the solutions for model parameters, including the timing of the ice movements and the observations of sea-level change, refer to the same radiocarbon time scale. It has sometimes been suggested that the observational evidence should be referred to the sidereal (or uranium-thorium) time scale but this would require that all observations used to construct the ice sheet models are also referenced to this scale. Because all published Late Pleistocene ice models are based on the radiocarbon ages, this latter time scale will be retained here and on the assumption that over the periods under consideration here this time scale is linear compared with the sidereal time scale (see Bard et al., 1990) the use of the radiocarbon scale should lead to internally consistent results. The viscosity estimates will therefore be in units of Pa radiocarbon-seconds and in so far as the two time scales may differ by as much as 15% (Bard et al., 1990) this distinction is not altogether trivial.

3. Sea levels during Late Pleistocene and Holocene times

The variation of sea level over the past 20,000 years is conveniently discussed according to the epoch for which the observations or predictions are made; as the *glacial maximum* stage at about 20,000 to 18,000 years ago (20–18 ka BP) when the ice sheets reached their maximum extent, the *late-glacial* stage when the ice sheets were melting rapidly up to about 6 ka BP, and the *postglacial* stage from about 6 ka BP to the present. In addition to this temporal description it is also constructive to discuss the characteristics of sea-level change in terms of the position of the observation or prediction site relative to the margins of the former ice sheets (Clark et al., 1978). *Near-field* locations are defined as those that occur within the limits of the former ice sheets and include sites in the Hudson Bay close to the centre of the former Laurentian ice sheet and sites in the Gulf of Bothnia near the centre of the former Fennoscandian ice sheet. At these locations the dominant contribution to sea-level change comes from the ice-load term, and the characteristic relative sea-level curve following the onset of deglaciation is one of a quasi-exponential fall up to the present (Fig. 1a). For locations near the former ice margins, the *ice-margin* sites, the contributions $\Delta\zeta_i$ and $\Delta\zeta_e$ may be of a similar amplitude but of opposite sign, so that quite complex temporal and spatial patterns of sea-level change can develop. For these sites, such as along the coast of Norway, the sea-level change is characterised by an initially rapid fall in level during the late-glacial stage, followed by a period of relative stability at around 10 ka BP and then a rise in level up until about 6 ka BP. During the postglacial stage the level falls more or less uniformly to its present position (Fig. 1b). Because the ice-load term changes rapidly with distance from the ice sheet, the details of the sea-level curve can evolve rapidly even over rela-

tively short distances. Further away, where the magnitude of the ice-load term is less than that of the esl contribution, the sea-level curve resembles the eustatic curve but with the important distinction that the levels continue to rise relative to the crust even when deglaciation has ceased, albeit at a slower rate than during the late-glacial stage (Fig. 1c). Sites for which the sea-level curve has this characteristic shape, as along the coast of the Netherlands or the French Atlantic coast, will be referred to as *intermediate-field* sites. *Far-field* sites are defined as those well away from the influence of the former ice sheets, such as locations along the Australian margin or Pacific Ocean islands. Here sea-level change follows, in the first approximation, the equivalent sea-level function and generally $|\Delta\zeta|_w > |\Delta\zeta_i|$. Departures from the esl curve, while small, contain important information on both mantle and ice-sheet parameters. At these far-field continental margin sites, sea level since the time of the last glacial maximum is characterised by several features (Fig. 1d):

(1) a stationary or nearly stationary level at a depth of 130–140 m below present sea level which formed when the ice sheets were at their maximum limit;

(2) a rapid rise in sea level, at a rate of 10–15

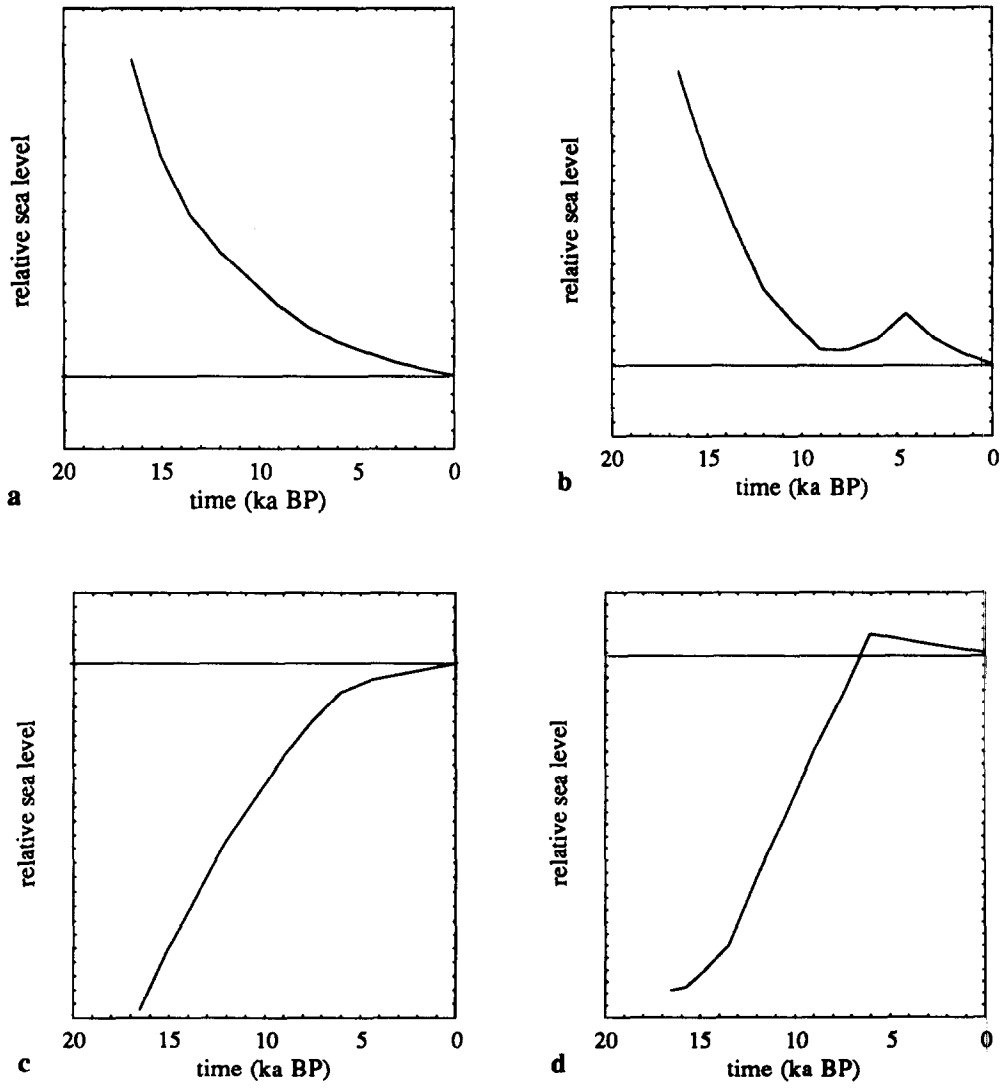

Fig. 1. Schematic representations of relative sea-level change at: (a) a site near the centre of the ice load; (b) a site within the ice sheet but near the margin; (c) an intermediate-field site; and (d) a far-field continental margin site.

m/ka, at the time the ice sheets melted and the ocean volume increased;

(3) the time at which sea level first reached its present value, before about 6 ka BP, when all melting ceased and after which a small highstand developed; and

(4) a nearly uniform fall in sea level from this highstand until the present time.

Observed far-field ocean-island sea-level curves are similar to these continental margin sites except that the highstand amplitudes are generally smaller and that they may occur a little later in time (e.g., Pirazzoli et al., 1988).

3.1. Sea levels during the last glacial maximum

Sea levels during the last glacial maximum in the far-field, while approaching the esl estimates,

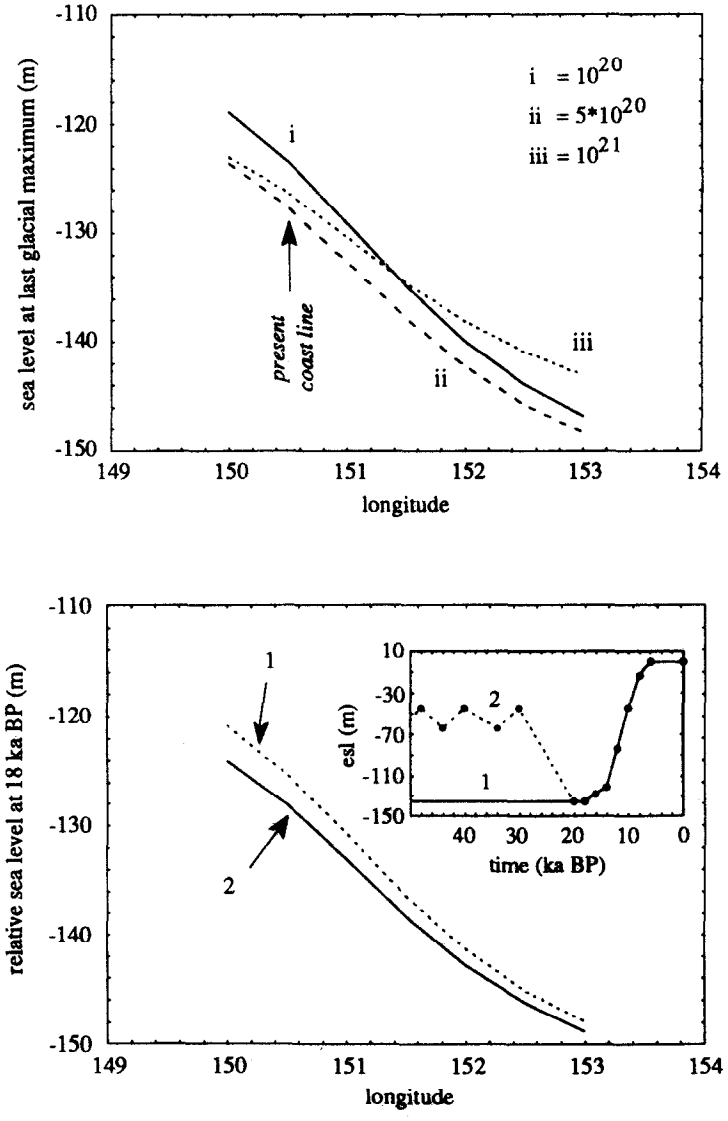

Fig. 2. (a) Predicted sea levels during the last glacial maximum at sites along a section of latitude 23.5°S across the Queensland coast for three earth models with different upper mantle viscosity, a lower mantle viscosity of 10^{22} Pa s and lithospheric thickness of 80 km. (b) Same as (a) but for the earth model (*ii*) and with two ice models (*1*, *2*) whose equivalent sea-level functions before 18 ka BP differ as shown in the inset.

are predicted to be regionally variable because of the contributions of the ice and water loads to the total sea-level change, and the observed sea levels for this period do not give a direct measure of the volume of melted ice. In particular, the glacio-hydro-isostatic model predicts that across continental margins this spatial variation may reach 20–30 m, depending on the adopted mantle viscosity profile (Fig. 2a) (Lambeck and Nakada, 1990) as well as, but to a lesser degree, on the duration of the maximum glaciation (Fig. 2b). (Models for far-field sites in which the maximum ice load persisted for very long periods tend to give a lower level at the start of melting than do models in which this ice load was short-lived because of the increased ocean basin volume created by the collapse of the peripheral bulge; see also section 3.3. below.) Observations of this lowest sea stand can therefore only be accurately related to estimates of the volume of the ice sheets for this epoch if the glacio-hydro-isostatic deformation of the Earth is taken into consideration.

Reliable measurements of this level from far-field locations are unfortunately few and not very reliable, but most indicate that it occurred at about 130–150 m below the present level (e.g., Carter and Johnson, 1986; Ota et al., 1981; Chappell and Shackleton, 1986; van Andel and Veevers, 1967) and that the volume of the non-floating ice at the height of the last glacial maximum exceeded the present volume by about (50–60) $\times$ 10^6 km^3. The comparable glaciological estimate for the northern hemisphere (but which may also be influenced by observational estimates of sea level at the time of maximum glaciation) range from 40×10^6 km^3 to 54×10^6 km^3 (Denton and Hughes, 1981). The far-field sea-level observations for this period clearly favour the maximum estimates although they do not identify the location of any additional ice loads required, other than it being far from the sites of observation used for these comparisons. For the intermediate-field locations, such as sites along the Atlantic or Gulf of Mexico coasts of the United States of America, the ice-load contribution to the total sea-level change may be greater than for the far-field region and any inferences of ice volumes from such observations would be more strongly dependent on assumptions made about

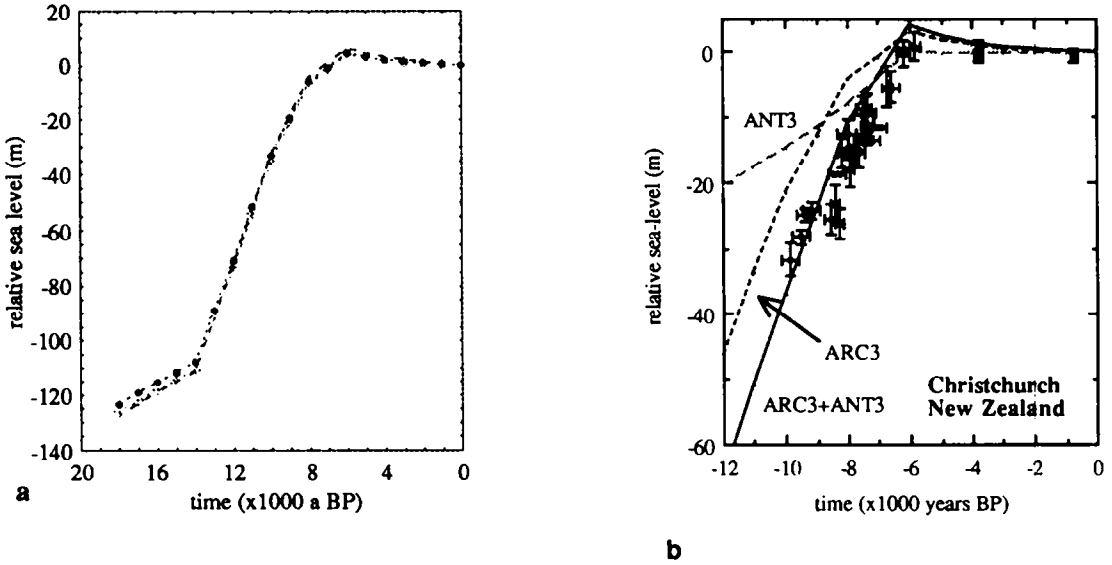

Fig. 3. (a) Predicted sea levels during the late-glacial stage at the Queensland coast at 23.5°S latitude, for the same three earth models as in Fig. 2(a). (b) Observed sea levels during the late-glacial stage at Christchurch, New Zealand, and the predicted sea levels for: (1) the northern hemisphere ice model ARC3 (including contributions from Laurentia, Fennoscandia and the Barents–Kara region); (2) the Antarctic ice model ANT3 (see Nakada and Lambeck, 1988); and (3) the combined ice model.

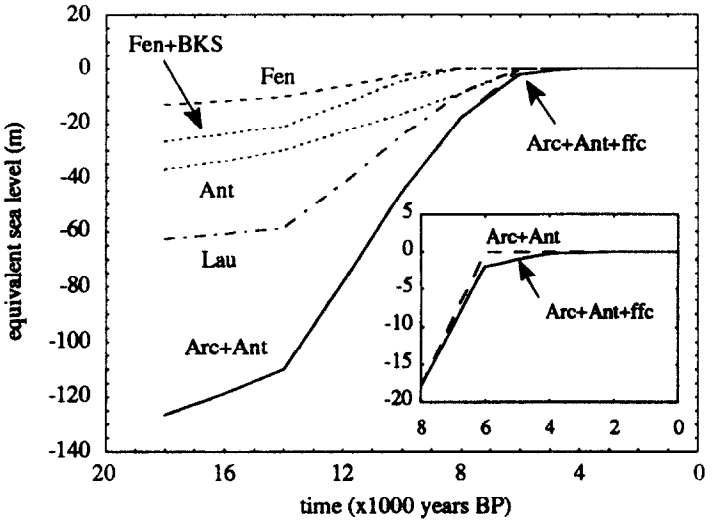

Fig. 4. The equivalent sea level (esl) functions for the component ice sheets, the total nominal esl function (Arc + Ant) and the corrected esl function (Arc + Ant + ffc) discussed below. Fen is the Fennoscandian contribution, BKS refers to an ice sheet model for the Barents and Kara Seas, Ant refers to the Antarctic contribution ANT3, and Lau refers to the Laurentide ice sheet. Fen + Lau correspond to the ICE1 model of Peltier and Andrews (1976) and Fen + Lau + BKS corresponds to the ARC3 model of Nakada and Lambeck. ffc is a far-field corrective term discussed in Nakada and Lambeck (1988).

both the ice sheet and earth model parameters than is the case for far-field sites.

3.2. Sea-level change during the late-glacial stage

In the far-field the eustatic rise in sea level after the onset of deglaciation is considerably greater than the water- and ice-load perturbation terms so that the predicted sea levels here are largely insensitive to mantle structure (Fig. 3a). Hence, far-field observations for the period up to the end of deglaciation at about 6 ka BP provide constraints on the global rates at which meltwater has been added into the oceans, as well as on the timing of this occurrence. If, as a starting model, the ARC3 model [based on the ICE-1 model of

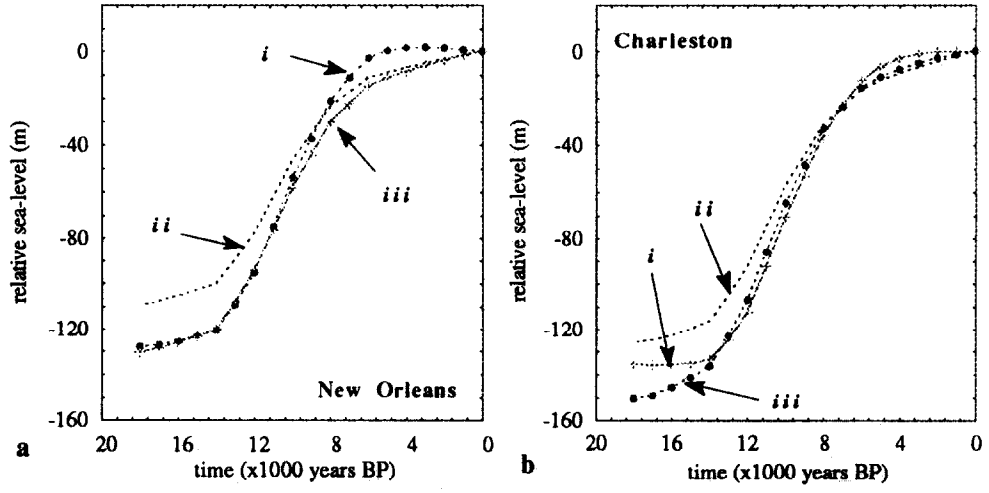

Fig. 5. Same as Fig. 3a but for two intermediate-field locations on (a) the Gulf of Mexico coast and (b) the North American Atlantic coast.

Peltier and Andrews (1976), which is a minimal ice volume model for Fennoscandia and Laurentia but to which an ice sheet over the Barents and Kara region of northern Europe has been added, see Fig. 4], is adopted, then some significant discrepancies occur between predictions and observations for the late-glacial stage (Fig. 3b) which can only be resolved by bringing forward the adopted melting histories by about 1000 years or by increasing the volume of melt-water that has been added into the oceans by about 30–40% (Nakiboglu et al., 1983; Nakada and Lambeck, 1987; see also Clark and Lingle, 1979). From the far-field observations alone it will not be possible to distinguish between these alternatives, although the observations of the sea level during the last glacial maximum at the far-field sites suggest that the latter option is preferable. At intermediate-field sites these late-glacial sea-level changes are more dependent on earth-model parameters than in the far-field (Fig. 5) because of the greater importance of the ice-load contributions in the former case and observations from such localities alone cannot be used to separate the ice- and earth-model parameters.

At near-field sites, the relative sea-level change during deglaciation is one of a fall in level at a rate that is a function of both the mantle rheology and the rate of ice decay. The minimum ice volume models such as ICE-1 predict late-glacial sea levels at sites in the Hudson Bay or in the Gulf of Bothnia that are generally in agreement with the observed values for a wide range of plausible earth models and they do not support solutions in which the thickness of the northern ice sheets is increased to the extent where the far-field discrepancies are removed (Quinlan and Beaumont, 1981; Nakada and Lambeck, 1988; Tushingham and Peltier, 1991). Nor do they support models in which the ice-melting history is brought forward by about 1000 years so as to resolve the discrepancy in the late-glacial part of the far-field sea-level curve. (Observations of sea level at about 6 ka BP in the far field and intermediate field in any case rule out this possibility as discussed below.) Thus, when combined with the far-field observations, the inference is that the additional ice originated from ice sheets away from the Laurentian and Fennoscandian localities. Possible locations are the wide continental shelves of northern Eurasia (the Barents and Kara Seas), Antarctica and possibly eastern Siberia (Grosswald, 1980; Denton and Hughes, 1981).

3.3. Sea level in mid- to late Holocene times

At about 6 ka BP the majority of the deglaciation had been completed and the great ice sheets of the northern hemisphere, with the exception of Greenland, had largely disappeared. Any sea-level change after this period is almost entirely a consequence of the ongoing adjustment of the Earth to the redistribution of the surface ice- and water-loads that occurred during the late-glacial phase. For the near-field localities, where the ice-load term dominates, this usually results in a continuation of the approximately exponentially decaying shore-line displacement curve with little, if any, change in the curvature, although for small ice sheets or for locations towards the edge of the ice sheet, where the ice-load term is reduced in amplitude, the termination of the global deglaciation can produce a change in gradient in the sea-level curve at this time. A prediction of this effect is seen in Figure 6 for sites along a profile across the ice margin in southern Sweden. For sites further away from the ice centre, the discontinuities become more pronounced and the timing of their occurrence provides strong constraints on the end of global melting of the ice sheets. However, at the ice-margin sites this relative highstand need not be a synchronous event, particularly at locations near the margin of ice sheets (such as Fennoscandia) whose melting was not in phase with that of the major ice sheet over Laurentia that dominates the equivalent sea-level contribution. Observations from sites in Norway and the Baltic region suggest an occurrence at about 6.5–6.0 ka BP while at the far-field continental margin sites these highstands usually occur at about 6 ka BP. These observations, therefore, preclude melting models in which the termination of deglaciation is brought forward considerably in time compared to the nominal equivalent-sea-level model adopted (Fig. 4) and support the

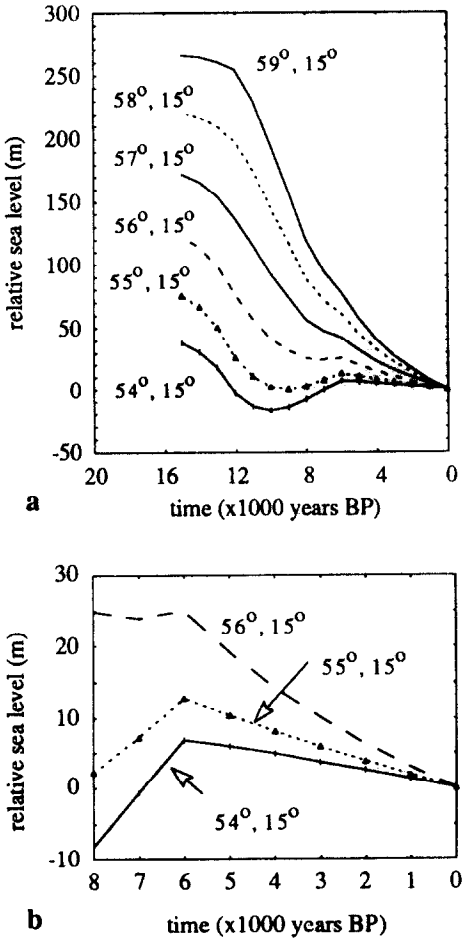

Fig. 6. Predicted sea levels for sites along a section at 15° east longitude through Sweden. The southern limit of the ice sheet at the time of maximum glaciation occurs at about latitude 54° north. These results are for the model (ii) defined in Figure 3a. Figure 6b gives the post-glacial results on an expanded scale for the more southern sites near the ice margin.

argument that the discrepancy in sea level for the late-glacial stage is a consequence of inadequate ice volume in the starting model rather than a result of the melting occurring later than assumed.

Figures 7a and 7b illustrate the sea-level curve observed at coastal locations in northern Queensland, Australia (see, for example, Chappell et al., 1983). Well defined highstands are observed at about 6.0 ka BP and other indicators of reef and shoreline development indicate that, prior to this time, sea level rose rapidly and first reached its present level at about or soon after 6.5 ka BP (Hopley, 1982). These mid-Holocene sea-level highstands are primarily the consequence of the loading of the sea floor by the meltwater in late-glacial time by which flow is induced in the mantle from beneath the ocean lithosphere to beneath the continental lithosphere, producing a tilting of the continental margin and shelf. Models of this primarily hydro-isostatic effect predict that the amplitudes of the highstand vary with coastline geometry and particularly with the distance of the site from the coastline. This is indeed observed: the amplitude generally decreases with increasing seaward distance from the coast and increases inland along the shores of narrow gulfs or tidal estuaries. The predicted amplitude of the highstand is also sensitive to the mantle structure, including the lithospheric thickness, and lateral structure across the continental margin may be important (Chappell et al., 1982). In particular, broad continental shelves with relatively thick lithosphere may impede the development of highstands along inland sites as appears to be the case in the Alligator River area of northern Queensland (Woodroffe et al., 1987) and along the Senegal River in west Africa (Faure et al., 1980).

Figure 7c illustrates the observed relative sea-level curve for a location in the upper Forth valley in Scotland (Sissons and Brooks, 1971). This also indicates a well-defined highstand at about 6 ka BP which is expressed throughout much of Scotland by raised beaches, platforms and marine sediment deposits (Sissons, 1983). Similar sea-level curves are observed along many sections of the Norwegian coast (e.g., Kjemperud, 1986; Svendsen and Mangerud, 1987). The predicted amplitudes of these mid-Holocene highstands, whether in the far-field or intermediate-field, are a function of the earth-model parameters, the geometry of the surrounding oceans into which the meltwater has been added, any residual ice unloading effects, and any departures from the assumed equivalent sea-level curve. Separation of some of these contributions is possible, particularly at the far-field locations, by examining differential amplitudes. Some of the predicted differential spatial variation at 6 ka BP is illustrated in Figure 8 for selected far-field sites. For the two South Australia locations of Port

Augusta and Cape Spencer where the observed differential highstands are about 2.5–3 m, the predicted difference in amplitude is primarily the result of the two sites being at different distances from the open ocean. Port Augusta, at the head of Spencer's Gulf, is effectively some 300 km inland whereas the Cape Spencer site is at the entrance to the gulf such that the warping of the continental margin by the water-load is much amplified at the inland site. Likewise, the difference in amplitude of about 1–1.5 m at 6 ka BP, observed between the two north Queensland localities illustrated in Figure 7, is a consequence of the different coastal geometries, with the Karumba site located in the southwest corner of the Gulf of Carpentaria and the Halifax Bay site located on the Coral Sea side of the Queensland coast. Provided that any eventual departures from the assumed equivalent sea level remain relatively small (otherwise iterative solutions may be required), the differential values for the highstands throughout the far-field region are largely independent of the assumed equivalent sea-level curve and are a function primarily of the adopted earth-model parameters. Hence, a separation of the parameters defining the Earth's response and those defining the global melting characteristics of the ice sheets becomes possible and, because the dominant contribution to the sea-level change is from the water-load term, the mantle parameters will correspond largely to the lithosphere and mantle of the region covered by the observations (Nakada and Lambeck, 1989).

An important property of the far-field sea-level curve for the postglacial period is the question of whether the fall in level to the present position is uniform, exponentially decreasing with time, or irregular. The predicted changes for the past few thousand years are generally less than 1 or 2 m so that precise observations of regional changes are

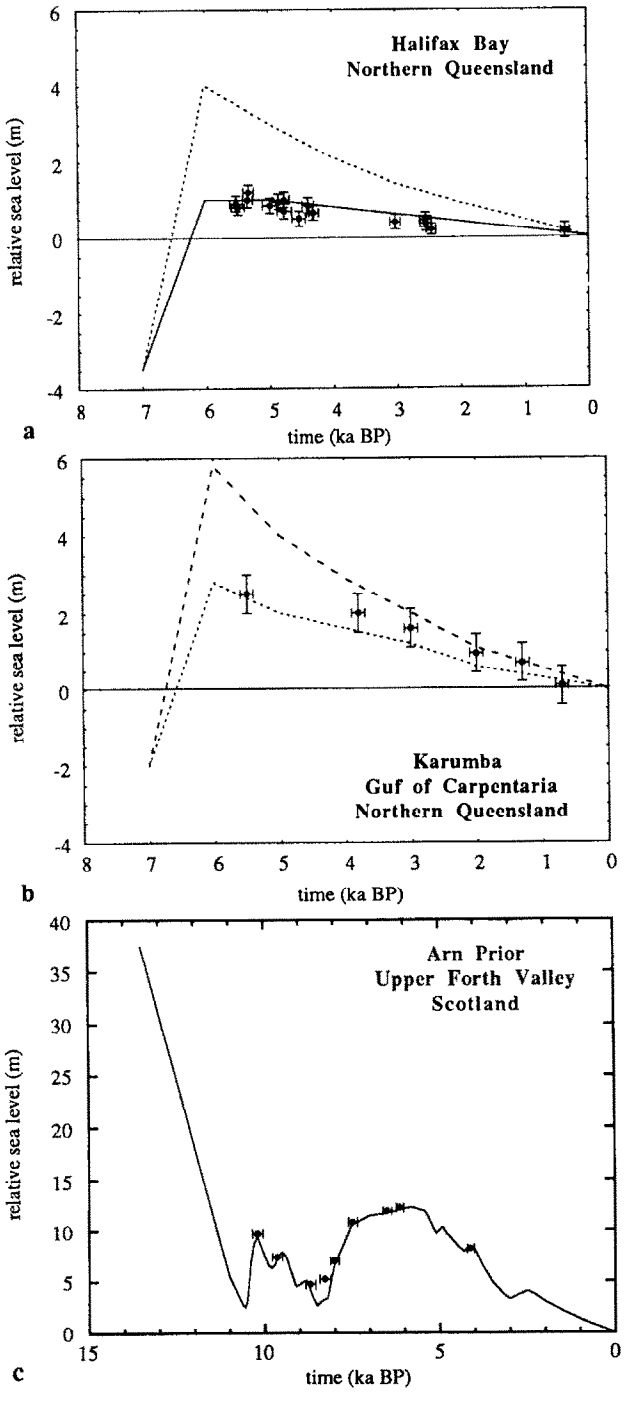

Fig. 7. Observed postglacial sea level at far-field locations in Queensland, Australia at (a) Halifax Bay, near Townsville, and (b) Karumba in the Gulf of Carpentaria (Chappell et al. 1983). (c) Late-glacial and postglacial sea level in the upper Firth of Forth valley, Scotland. Also illustrated in (a) and (b) are the predictions (dashed line) based on the parameters of the spatial differential observations (see below). The systematic difference between observations and predictions is an estimate of the correction $\Delta\zeta_e(t)$ to the equivalent sea-level function and the predictions corrected for this term are indicated by the solid line. The corrected esl is illustrated in Figure 4.

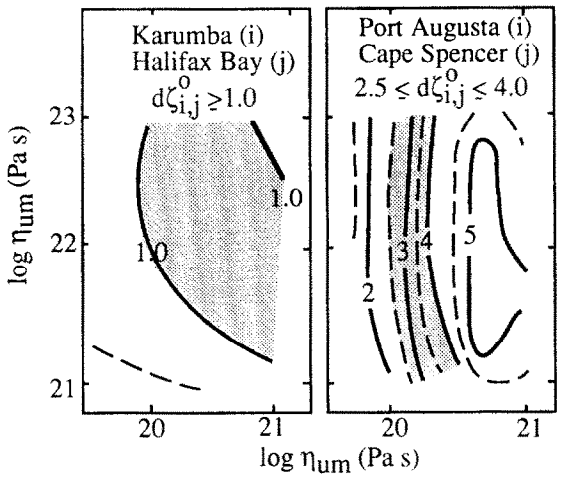

Fig. 8. Predicted differential sea levels for 6 ka BP between: (a) Karumba and Halifax Bay; and (b) Port Augusta and Cape Spencer.

difficult to distinguish from the background noise resulting from both the limitations of the past shoreline markers and any local perturbations. Nevertheless, the evidence from far-field continental margin sites suggests a nearly uniform decrease in sea level for the past 6000 years (e.g., Fig. 7; see also Chappell, 1983) and this can be used to provide some further constraint on the lithosphere and mantle rheology for the region. Certainly, these and similar observations from slowly emerging regions in the ice-marginal sites do not suggest that late Holocene oscillations in sea level are as significant as has sometimes been suggested (e.g., Ters 1986)

Because the predicted sea levels will be a function of possible changes in the volume of the Antarctica ice sheet, the mid-Holocene highstand amplitudes from southern latitude localities also contain information on possible changes in this ice sheet. This is illustrated in Figure 9 where an hypothesised contribution from an Antarctic deglaciation (the ANT3 ice model of Nakada and Lambeck 1988) results in a systematic trend in the ice-load term from north to south, whereas the corresponding arctic ice-load term is nearly constant over the region. Thus, if Antarctic ice volumes have been reduced significantly since about 18 ka BP, this could show up in a gradient of mid-Holocene highstand amplitudes from south to north. Such a trend is actually observed: highstands are absent from Tasmania, are small in southeastern Australia where the coastline is relatively linear in geometry, and tend, on average, to increase in amplitude northward along the Queensland coast (e.g., Hopley and Thom, 1983). Likewise, there is no strong evidence for mid-Holocene highstands in southern New Zealand, even in areas subjected to some tectonic uplift (e.g., Gibb, 1986).

Mid-Holocene highstands for ocean islands are usually much smaller in amplitude than those observed along the continental margins of the far-field. The sea-level response here has been likened to a dip-stick (Bloom, 1967) but this is only an approximate representation and other factors resulting from the complexities of the glacio-hydro-isostatic model must be considered (e.g., Mitrovica and Peltier, 1991). One modification of the dip-stick model is that the volume of the ocean basin evolves with time once deglaciation is initiated. Thus, the depressions formed around the ice sheets during the time of maximum glaciation relax and if these 'moats' occurred in an ocean environment, they lead to a reduction in the volume of the basin and to an increase in the sea level globally and sea level would rise faster than predicted by the equivalent sea-level effect. Similarly, the broad shallow bulges that are predicted to form beyond the ice sheet margins at the time of maximum glacial loading collapse as melting occurs and lead to an

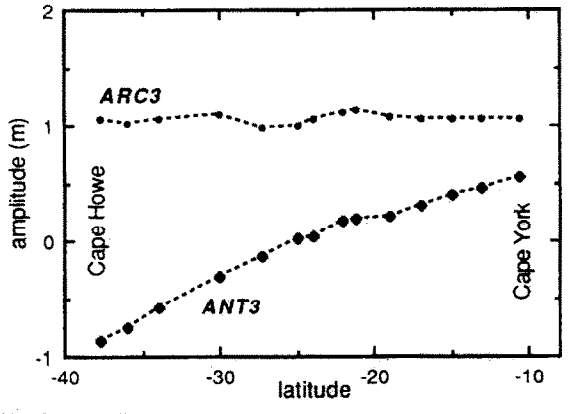

Fig. 9. Contribution at 6 ka BP to sea-level change Antarctic ice load along the eastern Australian margin from Cape Horne to Cape York for the Antarctic ice load term (ANT3) and the Arctic ice load term (ARC3).

increase in the ocean basin volume. Both contributions are small and are masked during the late-glacial stage by the eustatic changes but they become relatively more important during the post-glacial stage. As to which contribution, the 'moat' or 'bulge' effect, will be the dominant one depends on the positions of the ice sheet margins with respect to the continent outline, both at the time of the glacial maximum and during deglaciation. Generally, the bulge effect dominates and the high-resolution glacio-hydro-isostatic models predict mid-Holocene highstands for the ocean islands even when no meltwater is added to the oceans after 6 ka BP (e.g., Nakada and Lambeck, 1987; see also Mitrovica and Peltier, 1991; Johnston, 1993). The second departure from the dipstick response is caused by the island size: small islands move up and down with the sea floor but large islands, such as Hawaii or Viti Levu (Fiji), may be subject to differential movement compared with the surrounding sea floor if some flow of mantle material occurs from beneath the ocean lithosphere to beneath the island, similar to what happens beneath the continental margins (Nakada, 1986; Nakada and Lambeck, 1987). The mid-Holocene highstand amplitudes will also be a function of departures of the equivalent sea level from the assumed melting model but, like the continental far-field observations, spatially differential values for islands of different sizes will be mainly a function of mantle rheology and a separation of the various contributions to these high-

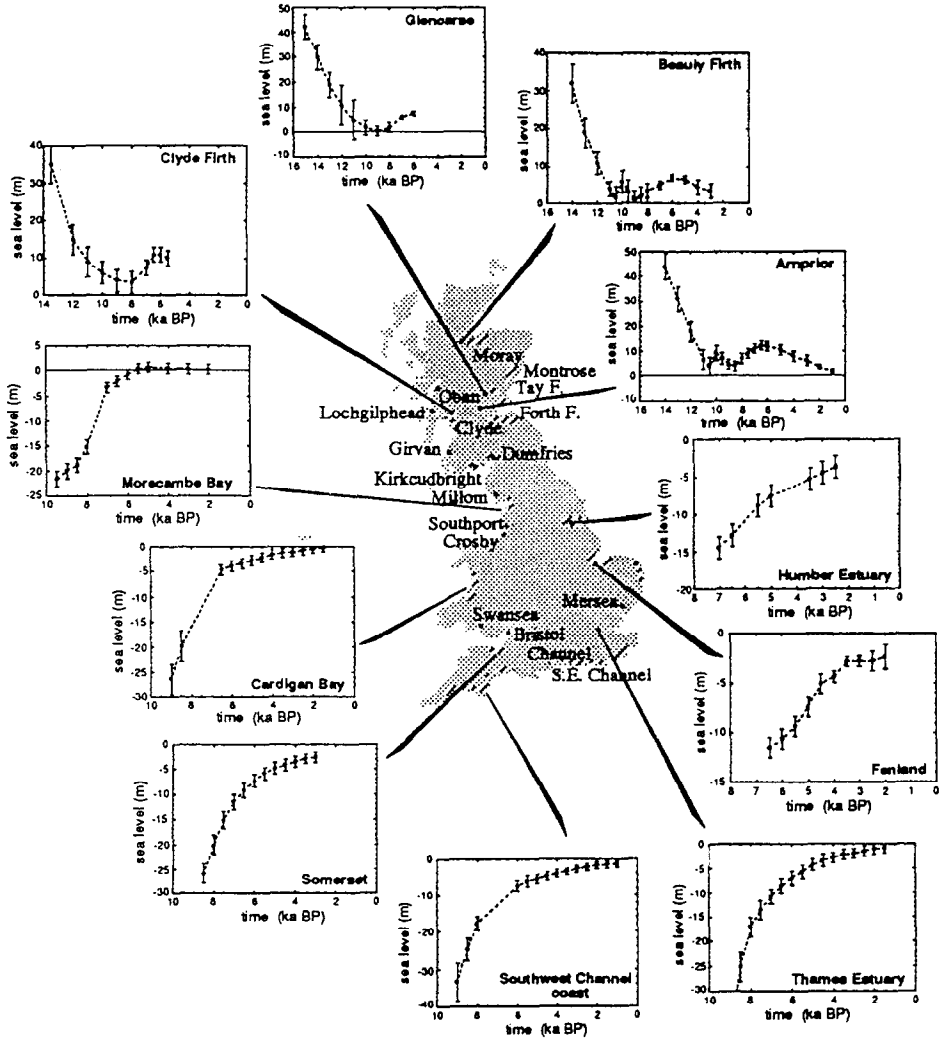

Fig. 10. Selected observed sea-level curves around the British Isles.

stands can be affected if accurate sea level data are available for tectonically stable islands.

In the case of intermediate- and near-field observations a similar separation of some of the ice-sheet and earth-model parameters is also possible. This is well illustrated by the observations of the rebound and associated sea-level change of the British Isles. Here, the sea-level curve is a combination of the local (i.e. British) rebound, the equivalent sea-level function from the much larger ice sheets, and lesser contributions from the water-load term and the ice-load terms associated with the Fennoscandian and Laurentian ice sheets. The actual sea-level change at any location will depend on the relative importance of these spatially variable contributions and considerable regional variability results, as is observed (Fig. 10). The limits and the subsequent retreat of the ice over the British Isles for the past 18–20 ka are reasonably well known over land but considerable controversy exists over the extent of the ice sheet over the offshore areas, particularly over the North Sea between Scotland and Norway. Here, because observations are well distributed around the limits of the former ice sheet as well as from near its centre thanks to the deeply penetrating sea-lochs, some separation of ice and earth parameters is again possible (Lambeck, 1991).

4. Results

A word of caution about the results obtained so far is appropriate in that they are dependent on models that still have some limitations or ambiguities including the use of first-iteration solutions in the far-field analysis, the assumption of non-adiabaticity in others, and the possibility of an incomplete definition of the model space in the inversions of the sea-level observations for earth- and ice-model parameters. Nevertheless, many of the conclusions reached appear to be robust and insensitive in other than detail to these earth-model limitations.

4.1. Earth models

The earth-model parameters to be determined from the observations of sea-level include the effective elastic thickness of the lithosphere and the effective (Maxwellian) viscosity of the mantle, with the latter parameter being depth dependent. The observation equation is (c.f. eq. 4):

$$\Delta\zeta_0(\varphi, \lambda : t) + \epsilon_0(\varphi, \lambda : t) = \Delta\zeta_e(t) + \delta\zeta_e(t) + \sum_{j=1}^{J} \beta^j \left\{ \sum_n \Delta\zeta_i^{(n,j)} + \sum_m \left(\Delta\zeta_w^{(m,j)} + \delta\zeta_w^{(m,j)} \right) \right\} \quad (5)$$

where:

$\Delta\zeta_0$ = the observed shoreline elevation (reduced to mean sea level) at location (j,l) and at time t for a total of S observations

ϵ_0 = estimation of the observation error

$\Delta\zeta_e$ = equivalent sea-level function for the totality of the ice sheets

$\delta\zeta_e$ = correction term to $\Delta\zeta_e$

β_j = scale parameter for the height of the jth ice sheet

$\delta\zeta_w^j$ = second order corrections to the water-load term, including the time dependence of the ocean geometry.

The general procedure for solving the S equations for the various unknown parameters has been to define the earth-model parameter space and predict sea levels for each model k ($k = 1,\ldots,K$) within this space and for each observation data point s ($s = 1,\ldots,S$). For an earth-model k the appropriate ice-model parameters are first estimated by searching through a defined ice-model parameter space for a combination of parameters that minimizes the quantity:

$$\sigma_k^2 = \frac{1}{S} \sum_{s=1}^{S} \left[\frac{\Delta\zeta_0^{(s)} - \Delta\zeta_{\text{predicted}}^{(s)}}{\sigma^{(s)}} \right]$$

where $\sigma^{(s)}$ is the standard deviation of the sth observation. The search is then conducted through the earth-model space K for the overall minimum variance.

The solutions have been conducted separately for several regions; for the far-field locations mainly from the Australasian region where the ice-parameter solved for is the corrective term $\delta\zeta_e$; for the British Isles, where the ice parameters include a scale factor for the heights of the British ice sheet as well as a corrective term for the equivalent sea-level function; for the Scandi-

navian region where the ice parameters include a scale factor for the Scandinavian ice sheet and $\delta\zeta_e$; and for the Barents–Kara Sea where the earth model is assumed known and equal to that established from the Scandinavian analysis and the sought parameters define the ice sheet over this region. For each regional solution, iterative procedures have been used when substantial changes to the starting ice models have been suggested from the comparisons with the observational sea-level data. For the far-field solution only the first-iteration solution has been considered, as has been the case for the preliminary solutions for the Barents Sea region. The other analyses are based on complete second-iteration solutions.

4.1.1. Earth-model parameters for the Australasian region

Only three-layer models have been considered here, comprising a lithosphere of effective elastic thickness H_l, an upper mantle of viscosity ν_{um} extending to a depth of 670 km and a lower mantle of viscosity η_{lm}. Only fully non-adiabatic solutions have been considered at this stage. The differential post-glacial sea levels are sensitive primarily to the upper mantle structure but some resolution for the lower mantle effective viscosity also occurs (e.g., Fig. 8). Taken together, the observations point to a significant increase in viscosity between the two mantle layers of from $(2–3) \times 10^{20}$ Pa s to about 10^{22} Pa s, although the uncertainty of the latter is relatively large. The optimum lithospheric thickness is about 80 km with some evidence for regional variation corresponding to the width of the continental shelf (Lambeck and Nakada 1990). Similar analyses for sea-level observations in the Pacific region, far away from the continents, point to lower values ($< 10^{20}$ Pa s) for the upper mantle viscosity (Nakada and Lambeck, 1989) although these solutions remain poorly constrained because of data limitations and the possibility of tectonic contributions to the apparent change in sea level.

4.1.2. Earth-model parameters for the British Isles

The glacial rebound calculations have been carried out for a high (25 km × 25 km) spatial resolution ice model defined at intervals of 500 to 1000 years, depending on the epoch from 22 ka BP to the end of the Loch Lomond glaciation at about 9 ka BP (Lambeck, 1993). Because of the relatively small dimensions of this ice sheet, the glacial rebound is primarily sensitive to the structure of the upper mantle, and models with more complex depth dependence of effective viscosity than used in the far-field analyses have been considered. Also, both adiabatic and non-adiabatic mantle models have been examined. Figure 11 compares the predicted ice-load components at a locality near Inverness relatively close to the centre of the former ice load for the two models with a three-layered mantle. The differences between the two results are relatively small, essentially because the surface load is composed largely of high wave-number terms whose corresponding viscoelastic Love numbers differ little for either the adiabatic or non-adiabatic assumption. Furthermore, the two models lead to results that are nearly linearly proportional to each other. Comparisons at other sites and for different earth-models, including mantle models with four viscosity layers, produce similar results and, for this region at least, a direct trade-off occurs between the degree of adiabaticity assumed and the scale factor β for the British ice sheet: Both the adiabatic and non-adiabatic solutions lead to the same viscosities but not the same β, with the latter leading to an underestimation of the ice height by about 10%.

Dependence of the predicted sea levels on lower mantle viscosity is generally not strong, although not negligible because the load spectrum, associated with the more distant ice sheets of Laurentia and Fennoscandia and with the water load, contains proportionally more power in low-degree terms than does the load spectrum for the British ice sheet. Initial tests with a three-layer model indicated that the minimum variances occurred when a substantial viscosity increase is introduced across the 670-km boundary with a value of about 10^{22} Pa s for the lower mantle (Lambeck 1993). Figure 12 illustrates the minimum variance estimates, based on a total of 424 observations of sea levels for the past 15,000 years, for the three-layer model with $\eta_{lm} = 10^{22}$

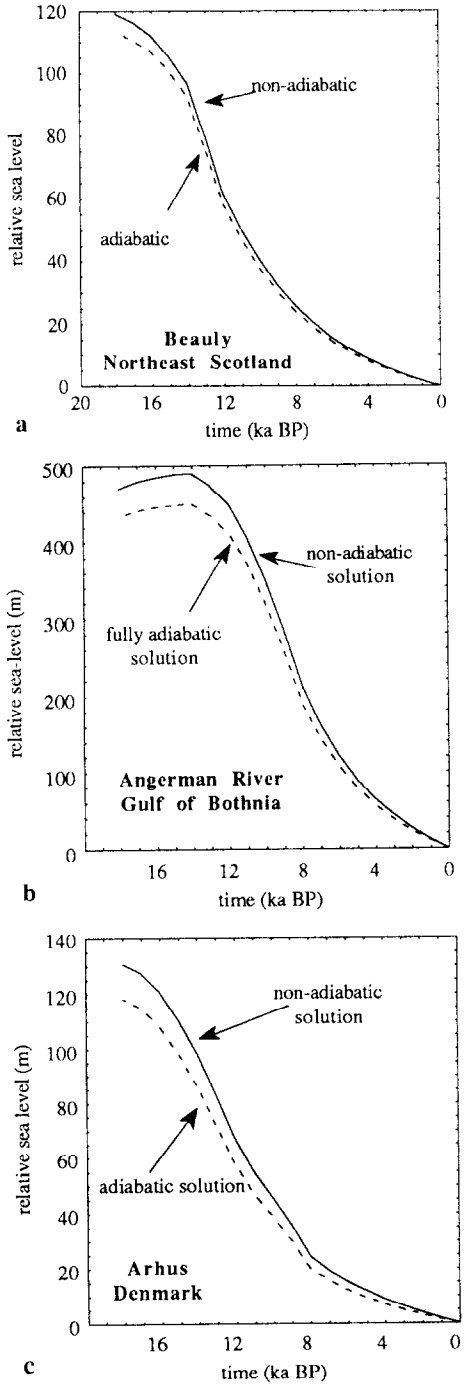

Fig. 11. Adiabatic versus non-adiabatic solutions for relative sea level for: (a) Beauly, northeastern Scotland and the British ice sheet only: (b) Angerman River, Gulf of Bothnia, near the centre of the Fennoscandian rebound, and the northern hemisphere ice sheets only; and (c) for northern Denmark, near the former ice sheet margin, and the northern hemisphere ice sheet only.

Pa s. For these three-layer models the optimum solution occurs for $H_l = 65$–70 km and $\eta_{um} = (4$–$5) \times 10^{20}$ Pa s. Results for models in which the upper-mantle layer is divided into two layers, corresponding to the mantle above the 400-km phase boundary and the transition zone, are illustrated in Figure 13 for $\eta_{lm} = 10^{22}$ Pa s and $H_l =$ 80 km. These results do not indicate that there is a marked depth dependence for the viscosity in the mantle above the 670-km seismic discontinuity. A further subdivision of the upper mantle to include a layer from the base of the lithosphere to a depth of 200 km also does not lead to strong evidence for an increase in mantle viscosity with depth from the base of the lithosphere to the 670-km boundary (Fig. 14). Furthermore, there is no support for models in which there is a pronounced narrow low-viscosity layer immediately below the lithosphere (Fig. 13b).

4.1.3. Earth-model parameters for northwestern Europe

The Scandinavian ice sheet at the time of maximum glaciation was considerably larger and will have stressed the mantle down to greater depths than the British ice sheet so that a comparison of effective viscosity profiles for the two regions may help resolve the depth dependence of the viscosity of the upper and middle mantle. The ice model used here is ARC-3 which is based on an interpolated version of ICE-1 of Peltier

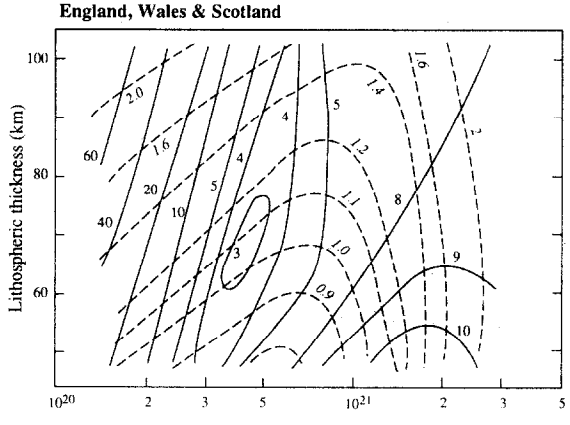

Fig. 12. Minimum variance solutions ($\sigma^{2,k}$) for the three-layer model with $\eta_{lm} = 10^{22}$ Pa s for the British Isles data set.

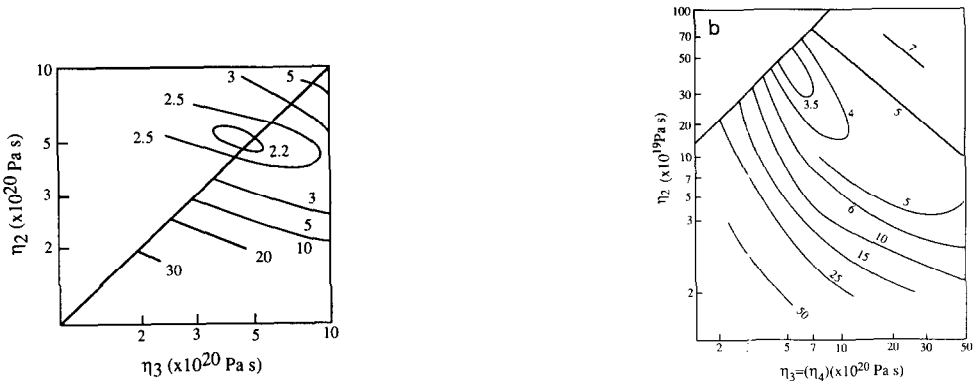

Fig. 13. (a) Minimum variance plots for the four-layer model with H_3 = 80 km and $\eta_{lm} = 10^{22}$ Pa s for the British Isles data set. (b) same as (a) but in which the upper mantle consists of a low-viscosity channel from 80 km to 200 km depth and a uniform viscosity from 200 to 670 km depth.

and Andrews (1976) and a schematic representation of the Barents–Kara ice sheet (Nakada and Lambeck, 1988). This model is relatively crude and not very appropriate for modelling the shoreline displacements at localities near the former ice margins, so that the comparison of observations and predictions is made only for sites that lie either near the centre of the ice sheet or well beyond the ice margins. Earlier results for the three-layer earth model based on the same ice model but a smaller observational data set (Lambeck et al., 1990) indicated the existence of a strong viscosity increase across the 670 km discontinuity and as this feature has been identified

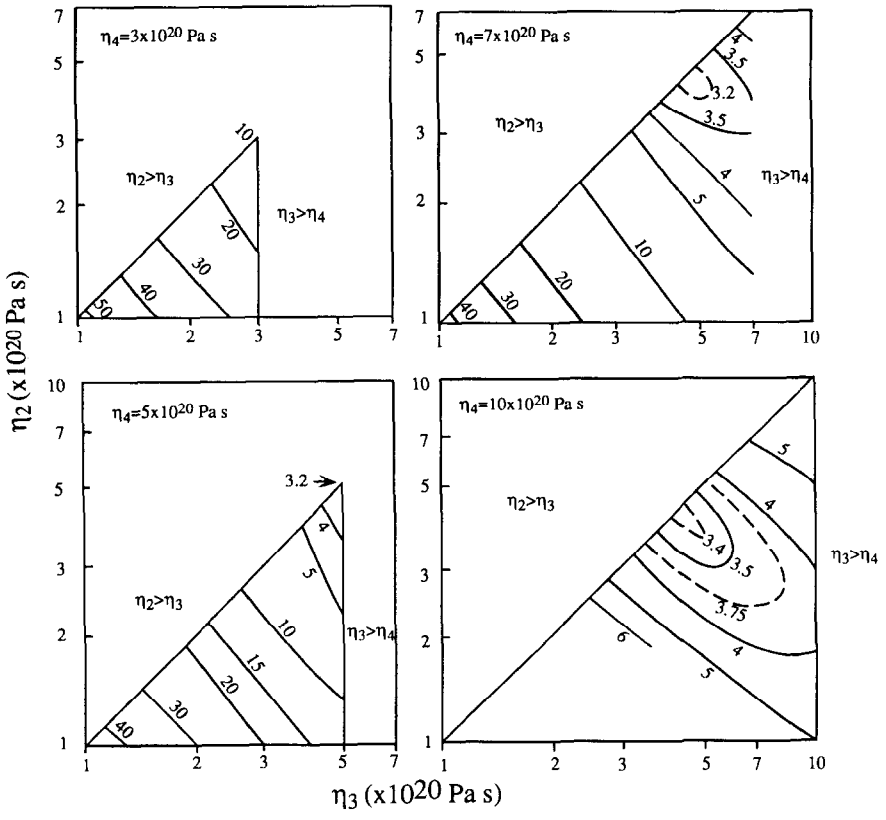

Fig. 14. Minimum variance solutions for the five-layer model with $\eta_{lm} = 10^{22}$ Pa s and $\eta_2 < \eta_3 < \eta_4$ for the British Isles data set.

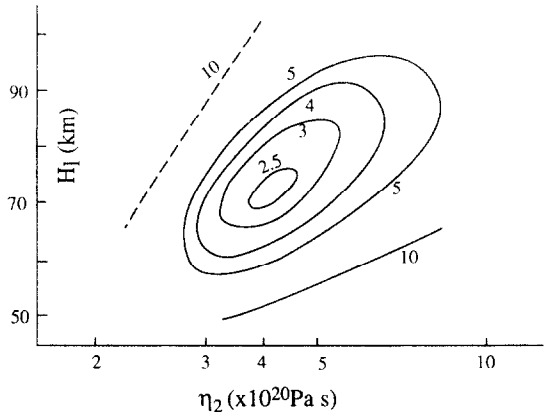

Fig. 15. Same as Fig. 12 but for the northwestern European data set.

in other regional analyses as well it has been retained here. New high-resolution ice-sheet models have been developed for both Fennoscandinavia and the Barents Sea and tested against a more comprehensive observational sea-level data set and these indicate that the results presented here give a reasonable description of the mantle response. Both non-adiabatic and adiabatic models have been examined and, as for the British

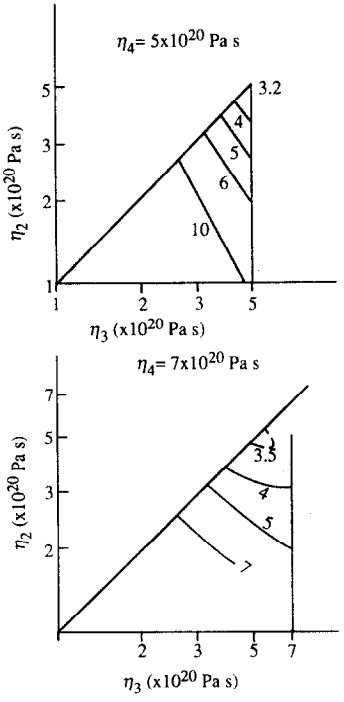

Fig. 16. Same as Fig. 14 but for the northwestern European data set.

Isles, the effect of the non-adiabatic assumption mainly leads to an underestimation of the scale parameter β for the ice heights by about 6% (Fig. 11). Figure 15 illustrates the minimum variance estimates for the three-layer solutions and the optimum solution occurs for about the same earth-model parameters as for the British solution. Results for the five-layer model are illustrated in Figure 16 and, as for the comparable British results, there is no strong support for earth models in which there is a pronounced viscosity gradient in the mantle above the 670-km discontinuity. Likewise, there is no support for the models with a pronounced low-viscosity layer immediately beneath the lithosphere as suggested by Fjeldskaar and Cathles (1991).

4.2. Ice model constraints: some conclusions

4.2.1. Ice volumes at 18–20 ka BP need to have been such that their melting raised global sea level by about 130–140 m.

This result is based on sea levels observed for the time of the last glacial maximum at sites in the far-field. The interpretation of such observations is not entirely unambiguous because it is earth-model dependent and because it also depends to some degree on the adopted ice model for the period before the maximum glaciation was reached. Relatively few observations for this period are available and those that do exist are generally not very accurate so that more precise constraints on the total ice volume are presently not possible. It will be important to obtain additional information, preferably away from continental margins such as to reduce the dependence on the assumptions about the earth model. Suitable sites for further investigation would be former small and shallow basins, now offshore at depths near and above about 140 m, which would have been isolated from a marine influence at the time of the last glacial maximum and which were transgressed by the sea soon after the onset of melting.

The ice sheet models for Laurentia and Fennoscandia consistent with the observed and predicted shoreline elevations generally have volumes that raise sea levels by only about 70 or 80

m so that the 'missing' ice volume must have been such as to increase sea level by about 50–60 m. The mismatch between observations and predictions at the far-field continental margin sites during lateglacial time and from widely separated locations in Australia, New Zealand, Japan and Malaysia (such as illustrated in Fig. 3b) support the conclusion that the northern hemisphere ice volumes are inadequate although improved observational evidence of late-glacial sea levels also is most desirable. Comparisons of sea-level obervations from near-field and ice margin sites with the glacio-hydro-isostatic rebound model results generally leads to a reduction in ice heights over the northern ice sheets compared with glaciological models, as is the case for studies of the Laurentide, Fennoscandia, and the British Isles (see below) and other locations for this 'missing' ice must be contemplated.

4.2.2. The ice sheet over Antarctica was greater than the present ice cover and its partial melting contributed significantly to the rise in sea level in lateglacial time.

Glacio-hydro-isostatic arguments that lead to this conclusion include the above 'missing' ice arguments as well as the observation of a general progression of the Holocene highstand amplitudes from south to north along the Australian eastern margin and the apparent absence of such highstands at the latitudes of Tasmania. Critical observations from tectonically stable regions further south are missing, although important new evidence comes from the Vestfold Hills area of the Antarctic continent where ice-free conditions have been preserved at least since late-glacial times. Sea-level change, predicted here on the assumption that Antarctic ice volumes have remained constant, are similar to those predicted at other far-field continental margin sites with the development of a small highstand at about 6 ka BP and levels below the present value at earlier times. However, observations from this region indicate that sea levels in mid-Holocene times were considerably higher than this and that the sea-level changes here are characteristic of the ice-margin sites of the northern hemisphere. Figure 17 illustrates results obtained for this area

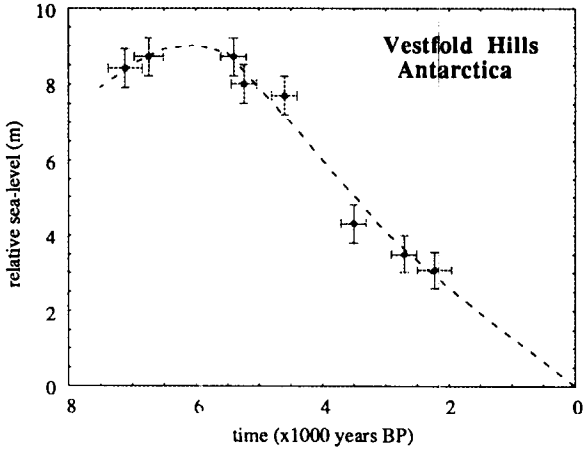

Fig. 17. Observations of isolation ages and heights of lakes in the Vestfold Hills, Antarctica (from D. Zwartz, M. Bird, J. Stone and K. Lambeck).

based on an analysis of sediment cores taken from lakes in the region and the results are similar to those observed from coastal localities of Norway that were within the ice sheet margin at the time of maximum glaciation. These ice-margin sea-level curves are primarily the sum of the esl and ice-load contributions that are of opposite sign and the occurrence of raised shorelines before 6 ka BP implies that there has been a substantial reduction in ice volume in lateglacial time. Reliable observations along the Antarctic margin are few and it is not possible to determine from these observations alone whether the Vestfold Hills sea-level curve is the result of a removal of local ice or a removal of larger amounts but more distant ice.

A tentative conclusion reached by Nakada and Lambeck (1988) from a comparison of late-glacial predicted and observed sea levels is that this 'missing' meltwater may actually have lagged behind the melting of the northern hemisphere ice sheets by about 1000 years, although improved observations for the late-glacial period are desirable in order to substantiate this interpretation.

4.2.3. Antarctic melting did not cease at 6 ka BP but a small amount of melting continued into more recent time

This conclusion is based on the use of differential amplitudes of the mid-Holocene highstand at far-field continental margin sites to estimate

mantle viscosity and the highstand amplitudes themselves to estimate the contribution from any changes in equivalent sea level (Nakada and Lambeck 1989). Figure 7 illustrates some typical results for northern Queensland sites where spatial differential sea levels have been used to estimate the best-fitting earth-model parameters. Any systematic discrepancies between the predicted and observed highstands, with the former based on the parameters derived from these differential observations, then provides a measure of the correction to the nominal equivalent sea-level function adopted. A generally consistent picture emerges for this far-field correction not only from the Australasian data but also from analyses for sea-level change in Great Britain and northern Europe (the $\Delta\zeta_e$ term in eq.4) and it appears that during the past 6000 years sea levels rose globally by some 2 or 3 m. The observation that the mid-Holocene highstands at far-field ocean island sites generally tend to be small, to occur later than 6000 a BP and to remain at a nearly constant level for up to 3000 years (e.g., Pirazzoli et al. 1988), supports this interpretation. These results do not identify the source of the meltwater that has been added into the oceans during the late-Holocene interval but an obvious candidate, once it is admitted that change occurred there, is the Antarctic ice sheet.

4.2.4. A major ice sheet existed over the Barents Sea in Late Pleistocene (Late Weichselian) times which may have extended to the east over the Kara Sea

The extent of the Late Weichselian ice sheet over the Barents Sea has been a subject of much debate with views ranging from only local ice sheets over the archipelagos of the arctic islands (Boulton, 1979) to a major ice sheet grounded on the shallow sea floor of the Barents and Kara Seas, coalescing with the ice sheet to the south and with a volume rivaling that of the Fennoscandian ice sheet (Grosswald, 1980; Denton and Hughes, 1981; Elverhøi and Solheim, 1983). Direct evidence for grounded ice sheets in Late Weichselian times has not been presented although the pattern of the emergence curves for the region strongly suggests that an extensive ice sheet existed over the Barents Sea in that period. Most views now favour the existence of a major ice sheet over at least the Barents Sea and the recent debate is largely focussed on the extent of the ice sheet at the time of maximum glaciation, on the location and relative importance of the different ice domes and ice fronts, on the duration of the glacial maximum and on the deglaciation history in latest Pleistocene and Holocene time (Solheim et al., 1990). The above conclusion is based on the observations of raised shorelines at numerous sites mainly located on Spitsbergen, Kong Karls Land, Nordaustland and Novaya Zemlya where shorelines of Late Weichselian and early Holocene ages have been identified at elevations from 50 to 200 m (e.g., Hoppe et al., 1969; Andersen, 1981; Salvigsen, 1981; Landvik et al., 1987; Forman, 1990). A comparison of these observations with simple models for ice sheets over the region indicates that a substantial ice sheet covered the Barents Sea and extended across the Kara Sea if the observations reported for Novaya Zemlya by Andersen (1981) are valid. The thickness of this ice sheet reached about 2500 m at the time of maximum glaciation. Also in order to match the various observations for western Spitsbergen the ice sheet extended out to the continental shelve along its western margin, consistent with recent results by Mangerud et al. (1992). These results will be discussed elsewhere.

4.2.5. The maximum ice thickness over Great Britain is unlikely to have exceeded about 1500 m at the time of maximum glaciation and this ice sheet did not extend across the North Sea to Norway after about 20 ka BP

This conclusion is based on the inversion of observations of sea-level change made around the British Isles (Lambeck, 1993). The observational evidence exhibits a complex spatial and temporal pattern for sea-level change which constrains well the rebound-model parameters defining both the Earth's rheology and the maximum ice volume. The limits of the British ice sheet over land are reasonably well established from geomorphological indicators but the limits over the adjacent ocean regions are poorly understood. In particular there has been considerable debate about the

extent of the ice sheet over the North Sea in Late Weichselian times but models such as those of Boulton et al. (1977) and Denton and Hughes (1981), in which the ice sheet at the time of the last glacial maximum extended across the North Sea to join up with the Norwegian ice sheet, predict that the centre of the late-glacial rebound is over northeastern Scotland, rather than over central Scotland as suggested by the observational evidence (e.g., Sissons, 1983). This therefore rules out such ice model unless the North Sea ice vanished well before about 20 ka BP (Lambeck, 1991). Estimates of the maximum thickness of the ice sheet over the British Isles have varied from about 1400 m (Boulton et al., 1985) to nearly 2000 m (Boulton et al., 1977), but inversion of the sea-level observations indicates that the optimum solutions require that the ice thickness over central Scotland is unlikely to have exceeded about 1650 m for the adiabatic model or about 1500 m for the non-adiabatic solutions. Estimates of this thickness over Ireland at the time of the last glacial maximum are less well constrained, largely because of the generally unsatisfactory nature of the late-glacial sea-level data from the Irish coast but initial results indicate that this was unlikely to have exceeded about 700 m.

4.2.6. The maximum ice thickness over Scandinavia is unlikely to have exceeded about 2500 m at the time of maximum glaciation

The ARC-3 model for Fennoscandia has a maximum ice thickness of 3000 m at the time of the last glacial maximum (Peltier and Andrews 1976) and this compares well with the model by Denton and Hughes. The preliminary inversions of the shoreline displacement data for both mantle and the ice parameters indicates scale factors β of about 0.80 for the minimum variance solution for the non-adiabatic models and 0.85 for the corresponding adiabatic model. Both results exclude larger ice volumes as would be required if part of the "missing ice" were to be introduced by increasing the Scandinavian ice heights at the time of maximum glaciation. If anything, these results suggest that the maximum ice heights over Fennoscandinavia are unlikely to have exceeded about 2500 m at the time of the last glacial maximum, but more than suggested by Nesje and Dahl (1990) from an analysis of rock weathering limits (but see Follestad (1990) for an alternate interpretation of the same evidence).

5. Conclusions

This symposium is concerned with issues of the relationship(s) between mantle processes and geological processes at/or near the surface of the Earth. One example of such a relationship that has been discussed in this paper is the surface adjustment to changing surface loads produced by the growth and decay of ice sheets and the concomitant changes in sea level: The redistribution of the surface load results in a redistribution of mass within the Earth and a deformation of the surface, the observation of which provides constraints on both the Earth's response function and on aspects of the ice load. One important aspect of this relationship that has not been discussed here is how this response can actually influence the extent of the ice sheets at the time of their maximum growth. By depressing the crust beneath the ice load, larger ice sheets can be supported, all other parameters controlling ice dynamics being equal, than would be the case if the Earth behaved as a rigid body such that low-viscosity mantle models can support larger ice sheets than can high-viscosity models. Purely glaciologically based models of the ice sheets do make assumptions about the Earth's response to ice loading so that there is a risk in the rebound modelling that the inferred earth-model parameters are merely those adopted in the glaciological model. An integrated glaciological-geophysical model is ideally required.

While many of the conclusions drawn here are of a preliminary nature, they do point to a need for improved observational data from key sites at different geographic locations and for different times. For example additional far-field sea levels during the glacial maximum and late-glacial stages is important, as is Holocene sea-level data from the Antarctic margin and tectonically stable southern latitude sites. Holocene highstands along the South American and African coasts would

also be beneficial in defining both the Antarctic contributions to the global ice volume balance and the regional variation in the Earth's structure.

References

Andersen, B.G., 1981. Late Weichselian ice sheets in Eurasia and Greenland. In: G.H. Denton and T.J. Hughes (Editors), The Last Great Ice Sheets. J. Wiley, New York, NY, pp. 1–65.

Bard, E., Hamelin, B., Fairbanks, R.G. and Zindler, A., 1990. Calibration of the ^{14}C timescale over the past 30,000 years using mass spectrometric U-Th ages from Barbados corals. Nature, 345: 405–410.

Bloom, A.L., 1967. Pleistocene shorelines: a new test of isostasy. Geol. Soc. Am. Bull., 78: 1477–1494.

Boulton, G.S., 1979. Glacial history of the Spitsbergen archipelago and the problem of a Barents Shelf ice sheet. Boreas, 8: 31–57.

Boulton, G.S., Jones, A.S., Clayton, K.M. and Kenning, M.J., 1977. A British ice-sheet model and patterns of glacial erosions and deposition in Britain. In: R.W. Shotton (Editor), British Quaternary Studies: Recent Advances. Clarendon Press, Oxford, pp. 231–246.

Boulton, G.S., Smith, G.D., Jones, A.S. and Newsome, J., 1985. Glacial geology and glaciology of the last mid-latitude ice sheets. J. Geol. Soc., London, 142: 447–474.

Carter, R.M. and Johnson, D.P., 1986. Sea-level controls on the post-glacial development of the Great Barrier Reef, Queensland. Mar. Geol., 71: 137–164.

Cathles, 'L.M., 1975. The Viscosity of the Earth's Mantle. Princeton University Press, Princeton, NJ, 386 pp.

Chappell, J., 1983. Evidence for a smoothly falling sealevel relative to north Queensland, Australia, during the past 6000 years. Nature, 302: 406–408.

Chappell, J. and Shackleton, N.J., 1986. Oxygen isotopes and sea level. Nature, 324: 137–140.

Chappell, J., Rhodes, E.G., Thom, B.G. and Wallensky, E., 1982. Hydro-isotasy and the sea-level isobase of 5500 BP in north Queensland, Australia. Mar. Geol., 49: 81–90.

Chappell, J., Chivas, A., Wallensky, E., Polach, H.A. and Aharon, P., 1983. Holocene, palaeo-environmental changes, central to north Great Barrier Reef inner zone. BMR J. Aust. Geol. Geophys., 8: 223–235.

Clark, J.A. and Lingle, C.S., 1979. Predicted relative sea-level canges (18000 years BP to present) caused by late-glacial retreat of the Antarctic ice sheet. Quat. Res., 11: 279–298.

Clark, J.A., Farrell, W.E. and Peltier, W.R., 1978. Global changes in postglacial sea level: a numerical calculation. Quat. Res., 9: 265–298.

Denton, G.H. and Hughes, T.J. (Editors), 1981. The Last Great Ice Sheets. Wiley, New York, NY, 484 pp.

Elverhøi, A. and Solheim, A., 1983. The Barents Sea ice sheet – a sedimentological discussion. Polar Res., 1 (n.s.): 23–42.

Farrell, W.E. and Clark, J.A., 1976. On postglacial sealevel. Geophys. J., 46: 79–116.

Faure, H., Fontes, J.C., Hebrard, L., Monteillet, J. and Pirazzoli, P.A., 1980. Geoidal change and shore-level tilt along Holocene estuaries: Senegal River area, West Africa. Science, 210: 421–423.

Fjeldskaar, W. and Cathles, L.M., 1984. Measurement requirements for glacial uplift detection of non-adiabatic density gradients in the mantle. J. Geophys. Res., 89: 10,115–10,124.

Fjeldskaar, W. and Cathles, L.M., 1991. The present rate of uplift of Fennoscandia implies a low-viscosity asthenosphere. Terra Nova, 3: 393–400.

Follestad, B.A., 1990. Block fields, ice-flow directions and the Pleistocene ice sheet in Nordmøre and Romsdal, West Norway. Norsk Geol. Tiddskr., 70: 27–33.

Forman, S.L., 1990. Post-glacial relative sea-level history of northwestern Spitsbergen, Svalbard. Geol. Soc. Am. Bull., 102: 1580–1590.

Gibb, J.G., 1986. A New Zealand regional Holocene eustatic sea level curve and its application for determination of vertical tectonic movements. Bull. R. Soc. New Zealand, 24: 377–395.

Grosswald, M.G., 1980. Late Weichselian ice sheet of Northern Eurasia. Quat. Res., 13: 1–32.

Hopley, D., 1982. The Geomorphology of the Great Barrier Reef. Wiley-Interscience, New York, NY, 453 pp.

Hopley, D. and Thom, B.G., 1983. Australian sea levels in the last 15000 years: a Review. In: D. Hopley (Editor), Australian Sea Levels in the last 15000 years: a Review. JCU, Dep. Geography, Monogr. Ser., 3: 3–26.

Hoppe, G., Schytt, V., Häggblom, A. and Österholm, H., 1969. Studies of the glacial history of Hopen (Hopen Island), Svalbard. Geogr. Ann., 51A: 185–192.

Johnston, P., 1993. The effect of spatially non-uniform water loads on prediction of sea-level change. Geophys. J. Int. (in press).

Kjemperud, A., 1986. Late Weichselian and Holocene shoreline displacement in the Trondheimsfjord area, central Norway. Boreas, 15: 61–82.

Lambeck, K., 1991. A model for Devensian and Flandrian glacial rebound and sea-level change in Scotland. In: R. Sabadini, K. Lambeck and E. Boschi (Editors), Glacial Isostasy, Sea Level and Mantle Rheology. Kluwer Academic Publ, Dordrecht, pp. 33–62.

Lambeck, K., 1993. Glacial Rebound of the British Isles. II: A high-resolution, high-precision model. Geophys. J. Int. (in press).

Lambeck, K. and Nakada, M., 1990. Late Pleistocene and Holocene Sea-Level Change along the Australian Coast. Palaeogeogr. Palaeoclimatol. Palaeoecol. (Global and Planetary Change Section), 89: 143–176.

Lambeck, K., Johnston, P. and Nakada, M., 1990. Holocene glacial rebound and sea-level change in NW Europe. Geophys. J. Int., 103: 451–468.

Landvik, J.Y., Mangerud, J. and Salvigsen, O., 1987. The Late

Weichselian and Holocene shoreline displacement on the west-central coast of Svalbard. Polar Res., 5: 29–44.

Mangerud, J., Bolstad, M., Elgersma, A., Helliksen, D., Landvik, J.Y., Lønne, I., Lycke, A.K., Salvigsen, O., Sandahl, T. and Svendsen, J.I., 1992. The last glacial maxium on Spitsbergen, Svalbard. Quat. Res., 38: 1–31.

McConnell, R.K., 1968. Viscosity of the mantle from relaxation time spectra of isostatic adjustment. J. Geophys. Res., 73: 7089–7105.

Mitrovica, J.X. and Peltier, W.R., 1991. On postglacial geoid subsidence over the equatorial oceans. J. Geophys. Res., 96: 20053–20071.

Nakada, M., 1986. Holocene sea levels in oceanic islands: implications for the rheological structure of the Earth's mantle. Tectonophysics, 121: 263–276.

Nakada, M. and Lambeck, K., 1987. Glacial rebound and relative sealevel variations: A new appraisal. Geophys. J.R. Astron. Soc., 90: 171–224.

Nakada, M. and Lambeck, K., 1988. The melting history of the Late Pleistocene Antarctic ice sheet. Nature, 333: 36–40.

Nakada, M. and Lambeck, K., 1989. Late Pleistocene and Holocene sea-level change in the Australian region and mantle rheology. Geophys. J., 96: 497–517.

Nakada, M. and Lambeck, K., 1991. Late Pleistocene and Holocene Sea-Level Change: Evidence for Lateral Mantle Viscosity Structure? In: R. Sabadini, K. Lambeck and E. Boschi (Editors), Glacial Isotasy, Sea Level and Mantle Rheology. Kluwer Academic Publ., Dordrecht, pp. 79–94.

Nakiboglu, S.M., Lambeck, K. and Aharon, P., 1983. Postglacial sealevels in the Pacific: Implications with respect to deglaciation regime and local tectonics. Tectonics, 91: 335–358.

Nesje, A. and Dahl, S.O., 1990. Autochthonous block fields in southern Norway: implications for the geometry, thickness, and isostatic loading of the Late Weichselian Scandinavian ice sheet. J. Quat. Sci., 5: 225–234.

O'Connell, R.J., 1971. Pleistocene glaciation and the viscosity of the lower mantle. Geophys. J., 23: 299–327.

Ota, Y., Matsushima, Y. and Moriwaki, H., 1981. Atlas of Holocene sea level records in Japan, Japanese Working Group of Holocene Sea Level Project IGCP.

Peltier, W.R., 1974. The impulse response of a Maxwell Earth. Rev. Geophys., 12: 649–669.

Peltier, W.R. and Andrews, J.T., 1976. Glacial-isostatic adjustment – 1. The forward problem. Geophys J.R. Astron. Soc., 46: 605–646.

Pirazzoli, P.A., Montaggioni, L.F., Salvat, B. and Faure, G., 1988. Late Holocene sea level indicators from twelve atolls in the central and Eastern Tuamotus (Pacific Ocean). Coral Reefs, 7: 57–68.

Quinlan, G.M. and Beaumont, C., 1981. A comparison of observed and theoretical postglacial sea-level in Atlantic Canada. Can. J. Earth Sci., 18: 1146–1163.

Salvigsen, O., 1981. Radiocarbon dated raised beaches in Kong Karls Land, Svalbard, and their consequences for the glaccial history of the Barents Sea area. Geogr. Ann., 63A: 283–291.

Sissons, J.B., 1983. Shorelines and isostasy in Scotland. In: D.E. Smith and A.G. Dawson (Editors), Shorelines and Isostasy. Academic Press, London, pp. 209–225.

Sissons, J.B. and Brooks, C.L., 1971. Dating of early post-glacial land and sea level changes in the western Forth Valley. Nature Phys. Sci., 234: 124–127.

Solheim, A., Russwurm, L., Elverhøi, A. and Berg, M.N., 1990. Glacial geomorphic features in the northern Barents Sea: direct evidence for grounded ice and implications for the pattern of deglaciation and late glacial sedimentation. In: J.A. Dowdeswell and J.D. Scourse (Editors), Glacimarine Environments: Processes and Sediments. Geol. Soc. Spec. Publ., 53: 253–268.

Svendsen, J.I. and Mangerud, J., 1987. Late Weichselian and Holocene sea-level history for a cross-section of western Norway. J. Quat. Sci., 2: 113–132.

Ters, M., 1986. Variations in Holocene sea level on the French Atlantic coast and their climatic significance. In: M.R. Rampino, J.E. Sanders, W.S. Newman and L.K. Königsson (Editors), Climate: History, Periodicity and Predictability. Van Nostrand Reinhold, New York, NY, pp. 204–237.

Tushingham, A.M. and Peltier, W.R., 1991. Ice 3G: A new global model of Late Pleistocene deglaciation based upon geophysical predictions of postglacial relative sea level change. J. Geophys. Res., 96: 4497–4523.

van Andel, T.H. and Veevers, J.J., 1967. Morphology and sediments of the Timor Sea. BMR J. Aust. Geol. Geophys., 82: 1–73.

Walcott, R.I., 1972. Late Quaternary vertical movements in Eastern America: quantitative evidence of glacio-isostatic rebound. Rev. Geoph. Space Phys., 10: 849–884.

Woodroffe, C.D., Thom, B.G., Chappell, J., Wallensky, E., Grindrod, J. and Head, J., 1987. Relative sea level in the South Alligator River region, north Australia, during the Holocene. Search, 18: 198–200.

Wu, P. and Peltier, W.R., 1983. Glacial isostatic adjustment and free air gravity anomaly as a constraint on deep mantle viscosity. Geophys. J., 74: 377–450.